

Theoretical study of reactive melt infiltration to fabricate Co-Si/C composites

Saqib Shahzad, Khurram Iqbal, and Zaheer Uddin

Citation: Chin. Phys. B, 2021, 30 (**11**): 116102. DOI: 10.1088/1674-1056/abeee7
Journal homepage: http://cpb.iphy.ac.cn; http://iopscience.iop.org/cpb

What follows is a list of articles you may be interested in

Heredity of clusters in the rapidly cooling processes of Al-doped $Zr_{50}Cu_{50}$ melts and its correlation with the glass-forming ability

Dadong Wen(文大东), Yonghe Deng(邓永和), Ming Gao(高明), and Zean Tian(田泽安)
Chin. Phys. B, 2021, 30 (**7**): 076101. DOI: 10.1088/1674-1056/abea93

Nearly golden-ratio order in Ta metallic glass

Yuan-Qi Jiang(蒋元祺), Ping Peng(彭平)
Chin. Phys. B, 2020, 29 (**4**): 046105. DOI: 10.1088/1674-1056/ab773f

Ab initio molecular dynamics study on the local structures in $Ce_{70}Al_{30}$ and $La_{70}Al_{30}$ metallic glasses

F X Li(李福祥), J B Kong(孔吉波), M Z Li(李茂枝)
Chin. Phys. B, 2018, 27 (**5**): 056102. DOI: 10.1088/1674-1056/27/5/056102

Serrated magnetic properties in metallic glass by thermal cycle

Myong-Chol Ri(李明哲), Sajad Sohrabi, Da-Wei Ding(丁大伟), Bang-Shao Dong(董帮少), Shao-Xiong Zhou(周少雄), Wei-Hua Wang(汪卫华)
Chin. Phys. B, 2017, 26 (**6**): 066101. DOI: 10.1088/1674-1056/26/6/066101

Five-fold local symmetry in metallic liquids and glasses

M Z Li(李茂枝), H L Peng(彭海龙), Y C Hu(胡远超), F X Li(李福祥), H P Zhang(张华平), W H Wang(汪卫华)
Chin. Phys. B, 2017, 26 (**1**): 016104. DOI: 10.1088/1674-1056/26/1/016104

Theoretical study of reactive melt infiltration to fabricate Co–Si/C composites

Saqib Shahzad[1,†], Khurram Iqbal[2,‡], and Zaheer Uddin[1,§]

[1] Department of Physics, University of Karachi, Karachi, Sindh 75270, Pakistan

[2] College of Computer Science and Information Systems, Institute of Business Management (IoBM), Karachi, Sindh 75190, Pakistan

(Received 11 February 2021; revised manuscript received 3 March 2021; accepted manuscript online 16 March 2021)

Cobalt-silicon based carbon composites (Co–Si/C) have established a noteworthy consideration in recent years as a replacement for conventional materials in the automotive and aerospace industries. To achieve the composite, a reactive melt infiltration process (RMI) is used, in which a melt impregnates a porous preform by capillary force. This method promises a high-volume fraction of reinforcement and can be steered in such a way to get the good "near-net" shaped components. A mathematical model is developed using reaction-formed Co–Si alloy/C composite as a prototype system for this process. The wetting behavior and contact angle are discussed; surface tension and viscosity are calculated by Wang's and Egry's equations, respectively. Pore radii of 5 μm and 10 μm are set as a reference on highly oriented pyrolytic graphite. The graphs are plotted using the model, to study some aspects of the infiltration dynamics. This highlights the possible connections among the various processes. In this attempt, the Co–Si (62.5 at.% silicon) alloy's maximum infiltration at 5 μm and 10 μm radii are found as 0.05668 m at 125 s and 0.22674 m at 250 s, respectively.

Keywords: cobalt-silicon/carbon composites, Co–Si alloy, reactive melt infiltration (RMI), carbon preforms

PACS: 61.25.Mv, 47.70.Fw, 83.80.Ab **DOI:** 10.1088/1674-1056/abeee7

1. Introduction

Cobalt-silicon/carbon composites are lightweight and heat resistant, and show quite a resistance from wear and tear. They are the replacement of the conventional materials in aerospace, automobile and heavy industries. Co–Si/C composites have been successfully commercialized particularly for the protection of friction parts.[1–4] To study the RMI dynamics of these composites, the wetting behavior is vital, which is the intermolecular interactions between the liquid and solid. If the reactive melt does not wet the substrate ($\theta > 90^\circ$), the forced infiltration can also be performed.[5]

Unlike coating which is just an additional layer of a material onto a different material and involving the surface only, the RMI technique is much deeper, in which a liquid permeates into porous material and chemically reacts with the walls of the cavities, throughout the rise. This not only enriches the material but changes it into a composite by altering its chemical and physical features and capabilities. To ensure that there is no foreign contamination, a vacuum is very important so that the infiltration can occur without any disturbance. Usually, infiltration is performed using the matrix in molten form, meanwhile, many metals such as silver, nickel, cobalt, copper, magnesium, and aluminum are easily melted and handled as a liquid. These are used in metal matrix composite's production.[6–13]

The complexity of this technique makes it worthwhile due to its products. Many studies are currently in progress and new technologies and techniques are being achieved and developed in the pursuit of advanced materials. Figure 1 illustrates an experimental setup; describing the infiltration process within the capillary of the porous carbon performed by molten metal-silicon (M–Si) using a conventional furnace in a vacuum.[13,14]

To investigate the infiltration kinetics, study of this process is essential, by assuming that the formation of SiC at interface only depends on the Si content rather than C, the threshold activity, $a_{\mathrm{si}}\,(\mathrm{SiC})$, can be calculated using the following equations:[15–21]

$$\mathrm{Si\,(in\ liquid\ Co)} + \mathrm{C(s)} \rightarrow \mathrm{SiC(s)},$$
$$\Delta H = -48.9\ \left[\frac{\mathrm{kJ}}{\mathrm{mol}}\right], \tag{1}$$
$$a_{\mathrm{si}}\,(\mathrm{SiC}) = \frac{1}{a_{\mathrm{c}}^{\mathrm{metal}}} \exp\left[\frac{\Delta G_{\mathrm{f}}^{0}\,(\mathrm{SiC})}{RT}\right], \tag{2}$$
$$\Delta G_{\mathrm{f}}^{0}(T) = -113482\left[\frac{\mathrm{J}}{\mathrm{mol}}\right] + 37.4872\left[\frac{\mathrm{J}}{\mathrm{mol\cdot K}}\right] T\,[\mathrm{K}], \tag{3}$$

where $a_{\mathrm{c}}^{\mathrm{metal}}$ is the activity of C in liquid metal C, $\Delta G_{\mathrm{f}}^{0}(T)$ is the Gibbs energy in the formation of Si–C, T is the temperature, and R is the gas constant.

†Corresponding author. E-mail: sayyed.saqib@hotmail.com

‡Corresponding author. E-mail: khurramiqbal.nust@gmail.com

§Corresponding author. E-mail: zuddin@uok.edu.pk

© 2021 Chinese Physical Society and IOP Publishing Ltd

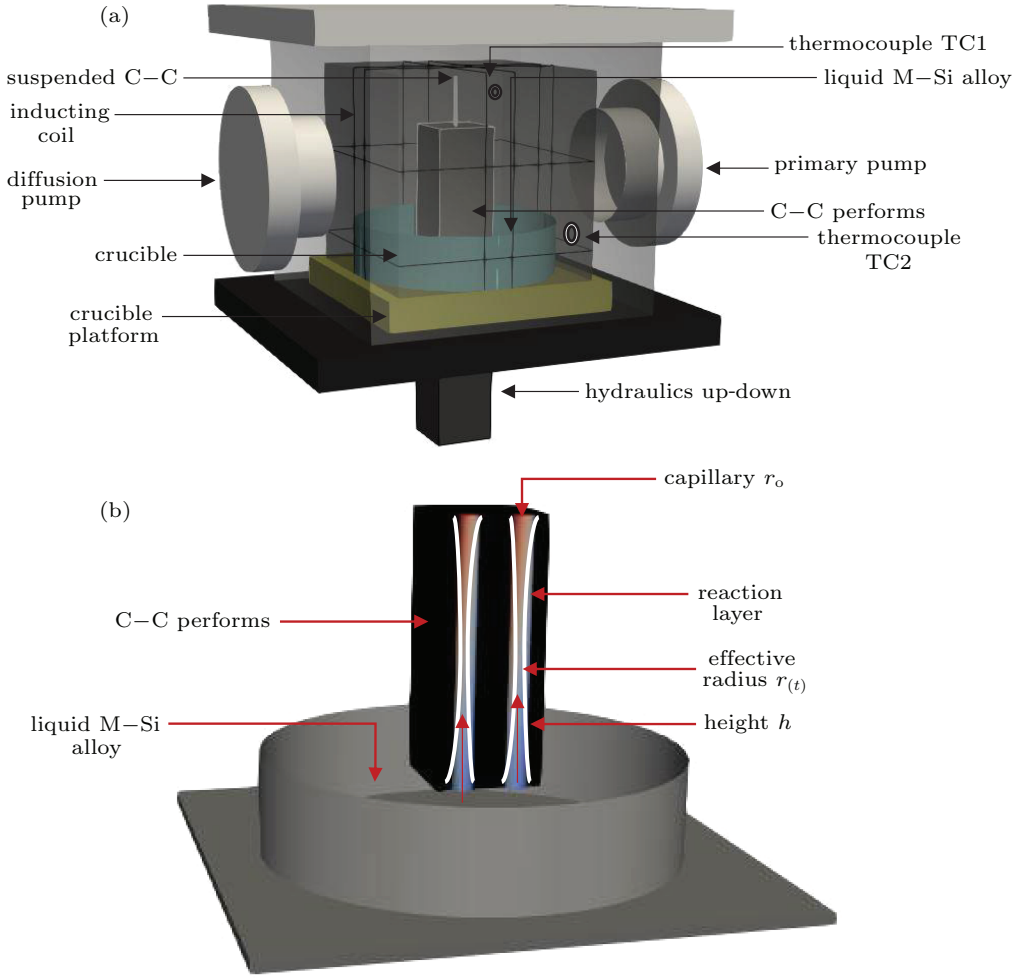


Fig. 1. Three-dimensional schematic diagram of (a) RMI experimental setup and (b) capillary-rise in the carbon perform (3D-view).

2. Infiltration process

The RMI techniques offer a dimension, which predicts the infiltration height, and the time to reach a certain or a desirable height. Theoretical models can determine the height of the infiltrant in a porous system. In this study, the "infiltrant" is liquid Co–Si and carbon is used as a porous system. The infiltration occurs when the reactive melt engages with the walls of the capillary (chemically combining throughout the impregnation); eventually fabricating the metal-silicon/carbon composite. The choking (termination) occurs in the Co–Si/C systems, as the melt rises to a certain height. The SiC formation results in a volumetric expansion leading to pore shrinkage. Theoretical calculations provide an insight into the experiment, helping in choice of the material (carbon performed) and the concentration of the metal alloys used for the impregnation. In this study, we discuss theoretical calculation on the desired metal-Si/C composite. Figure 2 illustrates a 3D-schematic diagram of the infiltration of liquid Co–Si into a carbon perform, with (a) the chocking of the moving front and (b) smooth infiltration. Since the silicon-carbon interface is responsible for the termination of the reaction, a time-dependent model is essential, which could predict the maximum impregnation before the termination occurs.

There is no doubt that the effectiveness, usefulness and fruitfulness of the Co–Si/C composites using RMI techniques are unparallel, and they can replace other materials that are being used in mechanical and aviation industries.

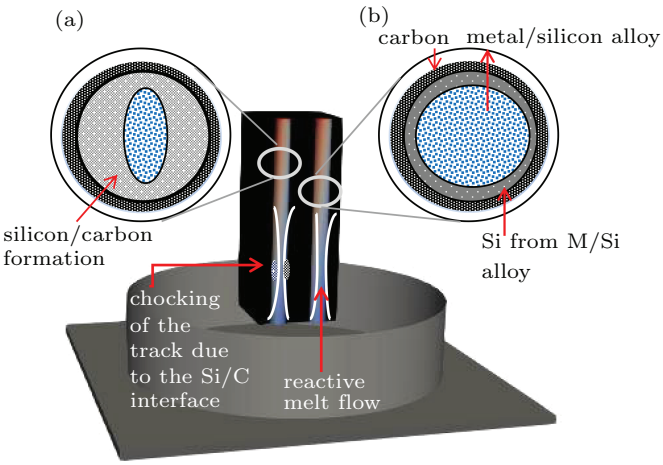


Fig. 2. Three-dimensional schematic diagram of (a) chocking of the capillary, (b) infiltration of reactive melt before the chocking (termination).

3. Numerical procedure

This research focuses on infiltration of Co–Si alloy front into porous carbon performs. Infiltration in the capillary is a distinctive "contact line" problem. Chibbaro *et al.*[22] revisited this issue with a basic model, also considering inertial effects, except the "vena contracta". The differential equation describing impregnation of the capillary by two fluids with the same density ρ, dynamic viscosity μ, and surface tension σ into a single channel in 2D reads[23,24]

$$\frac{\mathrm{d}^2h(t)}{\mathrm{d}t^2}+\frac{3\mu}{r^2\rho}\frac{\mathrm{d}h(t)}{\mathrm{d}t}=\frac{\sigma\cos\theta}{r\rho l}. \tag{4}$$

The opening term on the left-hand side speaks for inertial forces and the subsequent term represents the viscous forces. On the right-hand side the term is due to capillary action. Here r is the radius of the channel, h designates the position of the invading front, and l is the channel's length.

The models related to capillary action assume the process with a capillary of a uniform cross-section. If the wetting occurs, the liquid-vapor will develop a meniscus inside the capillary depending upon the pore size and contact angle. Across this meniscus, a capillary pressure will develop thus driving the liquid into the porous perform. Considering the hypothesis of a uniform cross-section of the bore, Calvimontes,[25] following Washburn,[22,26,27] developed an equation, describing the parabolic dependence of infiltration distance h on time t.

Furthermore, Einset[28] replaced the average radius by effective radius in the Washburn model, which gave even better success. Dullien *et al.*[29] extended the Washburn model to a real porous medium in which the effective channel radius was described by knowing the fact that in general the capillary should be considered for the varying cross-sections and the varying segments of a real porous medium. In this model (Eq. (4)) when inertial forces are neglected, for a shrinking radius, the radius is rewritten as $r(t)=r_0-kt$ (where r_0 is the initial radius and k is the reaction-rate constant). The estimated value of the reaction rate constant may be taken as $k\approx 4\times10^{-8}$ m·s^{-1}.[13]

A solution to Eq. (4) is given as

$$\frac{3\mu}{r^2\rho}\frac{\mathrm{d}h}{\mathrm{d}t}=\frac{\sigma\cos\theta}{r\rho l}, \tag{5}$$

$$\int_{h_0}^{h}\mathrm{d}h=\frac{\sigma\cos\theta}{3\mu l}\int r\,\mathrm{d}t, \tag{6}$$

$$\therefore\quad r=(r_0-kt), \tag{7}$$

$$h-h_0=\frac{\sigma\cos\theta}{6\mu kl}\left[r_0-kt\right]^2\Big|_0^t, \tag{8}$$

$$h(t)=\frac{\sigma\cos\theta}{6\mu kl}\left[(r_0)^2-(r_0-kt)^2\right]+h_0, \tag{9}$$

where h_0 is the initial position.

The two important parameters are the surface tension and viscosity for finding the infiltration height $h(t)$. To determine the surface tensions for specific temperatures and silicon percentages of the Co–Si alloy, Wang *et al.*[30] proposed that the surface tension of Co–Si alloy should be a function of both temperature (ΔT) and content of silicon (C) in cobalt-silicon alloy. As a result, the surface tension of the Co–Si alloy system can be inferred as

$$\begin{aligned}&\sigma(T,C)\\ &=1.882-1.12\times10^{-2}C\\ &\quad-\left(3.37\times10^{-4}+2.97\times10^{-6}C\right)\cdot\Delta T\ [\mathrm{N\cdot m^{-1}}],\end{aligned} \tag{10}$$

where $\Delta T=|1607-T|$ was experimentally suggested.[30]

The viscosities can be determined by the relation given by Egry[31] as follows:

$$\frac{\sigma}{\mu}=\frac{15}{16}\sqrt{\frac{kT}{M}}, \tag{11}$$

where k is Boltzmann's constant, T is temperature, σ is the tension, M is molecular weight, and μ is viscosity.

Based on Eqs. (10) and (11), Fig. 3 illustrates the surface tensions and viscosities calculated and extrapolated at different percentages of silicon in Co–Si alloy by keeping the temperature at 1723 K.

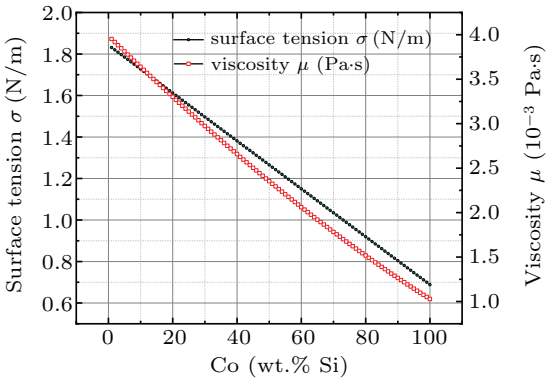


Fig. 3. Surface tension and viscosity of Co–Si alloy vs. silicon content.

4. Results and discussion

To calculate the infiltration height, experimental data is needed. Therefore, we choose the concentration (wt.% Si) for which the values of contact angles were known experimentally.[21,32] The contact angles (θ) can be calculated theocratically by[13,33]

$$\theta(t)=\theta_\infty+\theta_\infty\exp(B-A), \tag{12}$$

where A and B are material constants and θ_∞ is the equilibrium value of the contact angle.

The data from Table 1 show surface tension, viscosities and molecular mass calculated with the help of Eqs. (10) and (11). The carbon substrate used is the highly oriented pyrolytic graphite.[21,30,32]

Table 1. Data for cobalt-silicon wetting on carbon substrates at 1723 K.

Sample	Silicon content (wt.%)	Contact angle θ (°)	Surface tension σ (N/m)	Viscosity μ (mPa·s)	Absolute atomic mass M (kg)
1	32.2	120	1.4712	2.9029	8.1365×10^{-26}
2	62.5	< 15	1.1214	1.9905	6.5844×10^{-26}
3	75	40 ± 2	0.9771	1.6478	5.9442×10^{-26}
4	90	40 ± 2	0.8039	1.2651	5.1758×10^{-26}

The computational outcomes based on Eq. (9) are in Figs. 4 and 5, displaying the height of the reactive melt as a function of time and initial pore radius taken as $r_0 = 5$ μm and 10 μm. Material systems are studied at temperatures around 1723K for the Co–Si alloy. The infiltration kinetics depends on two factors: chemical reaction and properties of the liquid melt. The moving flow front shows an elliptical shape in the initial stage of the infiltration. As the process continues, the infiltration front encounters the conduit, the liquid melt gradually changes from a radial flow to a uniform flow due to the vena contracta. For given r_0 and k, time for the peak value remains the same for all concentrations:

$$t_{\max}(h) = \frac{r_0}{k} \quad \text{(time for maximum infiltration)}. \tag{13}$$

For a specific cobalt-silicon alloy, the larger radius ($r_0 =$ 10 μm) of the capillary yields more swift and larger infiltration height, than those for the smaller radius ($r_0 = 5$ μm). The nature of reaction in this system could take the form of dissolution, inter-metallic formation, or a combination of both processes. For this system, numerical studies provide the best prediction of optimal parameters for minimum conversion time.[14]

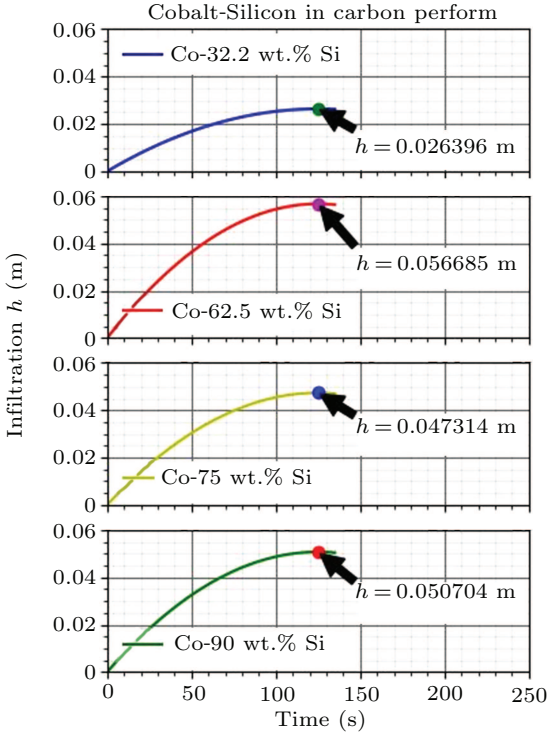


Fig. 4. Graphical outcomes of 32.2%, 62.5%, 75%, 90% of silicon content in Co–Si alloy infiltration with the capillary radius $r_0 = 5$ μm.

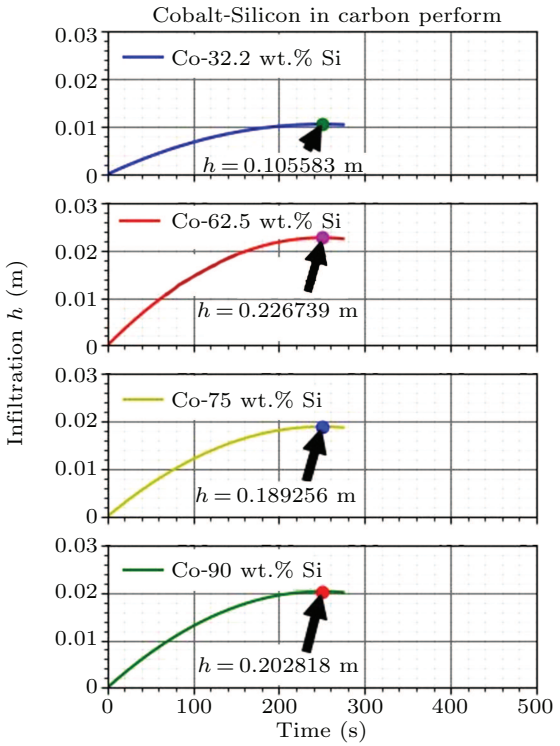


Fig. 5. Graphical outcomes of 32.2%, 62.5%, 75%, 90% of silicon content in Co–Si alloy infiltration with the capillary radius, $(r_0) = 10$ μm.

The greatest infiltration height is shown for the Co–Si alloy occurring at 62.5% of silicon. The infiltrations are 0.056685 m and 0.226738 m for 5 μm and 10 μm, respectively. The reason why the cobalt-silicon alloy with 32.2 wt.% Si has the lowest infiltration, only 0.026396 m and 0.105583 m for 5 μm and 10 μm, respectively, because of a higher contact angle (120°) that results in a lower wettability (weak solid to liquid interaction), higher surface tension (1.47 N/m) and higher viscosity (2.90 mPa·s), which creates resistance for the capillary action. On the other hand, the Co-75 wt.% Si and Co-90.8 wt.% Si alloys have the infiltrations of 0.047314 m and 0.050704 m for the capillary radius of 5 μm, respectively, and 0.189256 m and 0.202817 m for 10 μm, respectively. For a better understanding, a combined view is given in Figs. 6 and 7. In Fig. 6 the infiltration is shown after 25 s till 125 s, which is the time at which the infiltration is maximal for different percentages of Si content having the capillary radius of 5 μm. Similarly, In Fig. 7 the infiltration is shown after every 50 s till 250 s, which is the time at which the infiltration is maximal for different percentages of Si content having the capillary radius of 10 μm.

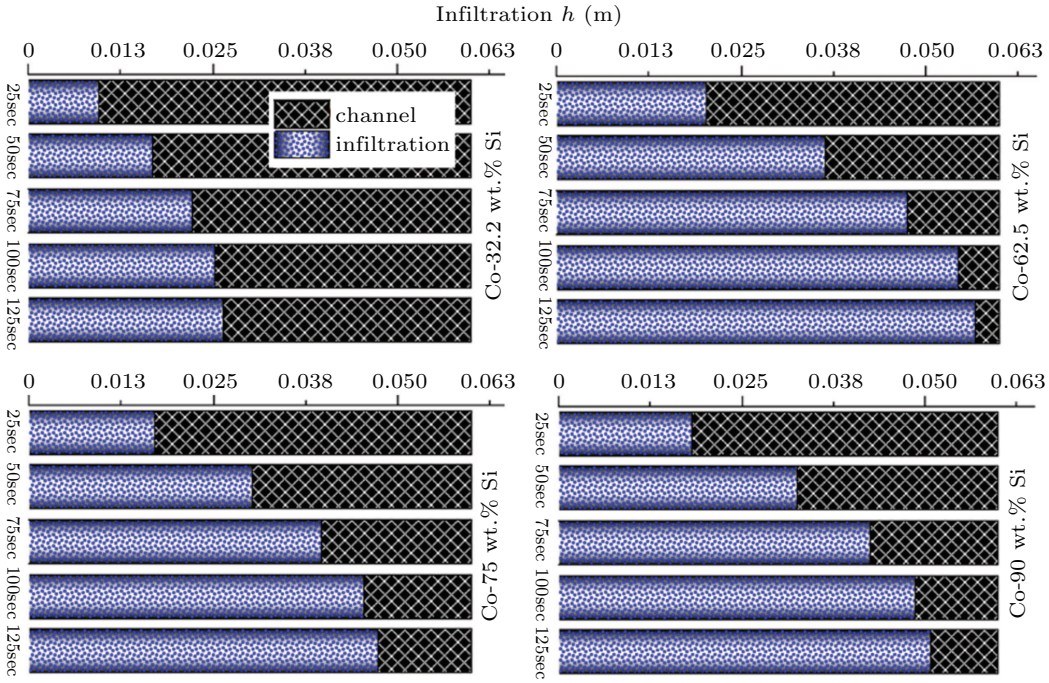


Fig. 6. Comparison of 32.2%, 62.5%, 75%, 90% of silicon content in Co–Si alloy infiltration with the capillary radius $r_0 = 5$ μm.

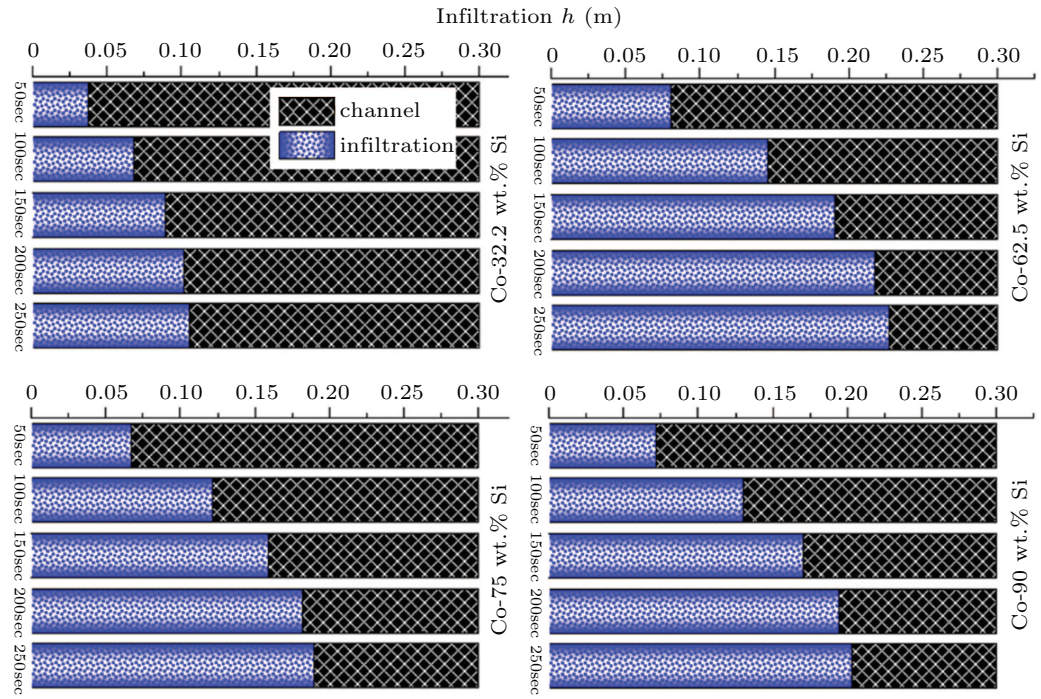


Fig. 7. Comparison of 32.2%, 62.5%, 75%, 90% of silicon content in Co–Si alloy infiltration with the capillary radius $r_0 = 10$ μm.

5. Conclusions

Carbon does not usually react with metal. To address this problem a silicon interface is used for effective bonding. In regarding this, a mathematical model is developed to represent the infiltration dynamics of the liquid-metal-silicon/solid-carbon system (Co–Si/C). The present model constitutes an important contribution to understanding of the highly dynamic process of liquid Co–Si infiltration on highly oriented pyrolytic graphite. This model is based upon the infiltration behavior of a single capillary system which is linked with the macroscopic infiltration dynamics. The advantage of the modeling is that it could provide an insight into the designing of Co–Si/C composites ranging over the desired parameters with minimal effort and allowing more precise optimization. The infiltration height depends upon the concentration of components of alloy and its temperature and wettability. In the above data, the infiltration heights are calculated at four different concentrations for given temperature and wettability. It

is found that the maximum infiltration height occurs for a concentration of 62.5 wt.% Si. For given wettability and temperature the time at which the maximal infiltration height occurs is the same, which implies that this time is independent of concentration.

The prospect of this study is to ensure a balanced percentage of cobalt-silicon alloys to have a good and effective infiltration so that a desirable Co–Si/C composite is fabricated for a desirable purpose. These composites have a variety of applications, enhancing the appearance, strengths, and other physical and chemical properties.

References

[1] Weng F, Yu H, Chen C and Dai J 2015 *Materials & Design* **80** 174
[2] Novakovic R, Giuranno D, Caccia M, Amore S, Nowak R, Sobczak N and Ricci E 2016 *J. Mol. Liquids* **221** 346
[3] Liu Y, Zhang Z, Xiao S, Qiang C, Tian L and Xu J 2011 *Appl. Surf. Sci.* **257** 7678
[4] Montgomery R S 1969 US Patent No. 3 454 375
[5] de Jongh, P E and Eggenhuisen T M 2013 *Adv. Mater.* **25** 6672
[6] Mortensen A 2000 *Comprehensive Composite Materials* **3** 521
[7] Takahashi M, Giuranno D, Ricci E, Arato E and Novakovic R M 2019 *Metall. Mater. Trans. A* **50** 1050
[8] Masoudi M, Hashim M, Kamari H M and Salit M S 2013 *Appl. Nanosci.* **3** 357
[9] Bahaaideen F B, Ripin Z M and Ahmad Z A 2010 *J. Sci. Industrial Res.* **69** 830
[10] Mizumoto M, Tajima Y and Kagawa A 2004 *Mater. Trans.* **45** 1769
[11] Vaezi M R, Sadrnezhaad K K and Nikzad L 2008 *Colloids Surf. A* **315** 176
[12] Bougiouri V, Voytovych R, Dezellus O and N Eustathopoulos N 2007 *J. Mater. Sci.* **42** 2016
[13] Iqbal K, Sha J J, Lei Z K, Maqsood A and Mujahid M 2014 *JOM* **66** 953
[14] Iqbal K, Dwivedi S and Cadet S 2018 *A Model for the Numerical Simulation of Liquid Silicon Infiltration into Porous Carbon/Carbon Preforms* in *Ceramic Transactions Series* Vol. 261 p. 23
[15] Kumar S, Kumar A, Mala R B and Mokhasunavisu R R 2015 *Int. J. Appl. Ceram. Technol.* **12** 176
[16] Srivastava V K 2012 *Am. J. Mater. Sci.* **2** 1
[17] Kumar S, Kumar A, Devi R, Shukla A and Gupta A K 2009 *J. Eur. Ceram. Soc.* **29** 2651
[18] Margiotta J C, Zhang D and Nagle D C 2010 *Int. J. Refrac. Met. Hard Mater.* **28** 191
[19] Sangsuwan P, Tewari S N, Gatica J E, Singh M and Dickerson R 1999 *Metall. Mater. Trans. B* **30** 933
[20] Fitzer E 1988 *Pure & Appl. Chem.* **60** 287
[21] Caccia M, Amore S, Giuranno D, Novakovic R, Ricci E and Narciso J 2015 *J. Eur. Ceram. Soc.* **35** 4099
[22] Chibbaro S, Biferale L, Diotallevi F and Succi S 2009 *Eur. Phys. J. Special Top.* **171** 223
[23] Sergi D, Grossi L, Leidi T and Ortona A 2016 *Engin. Appl. Computat. Fluid Mech.* **10** 485
[24] Sergi D Grossi L, Leidi T and Ortona A 2016 arXiv:1601.07697 [cond-mat.mtrl-sci]
[25] Calvimontes A 2018 *Preprints 2018, 2018020018*
[26] Washburn E W 1921 *Phys. Rev.* **17** 273
[27] Pan Y, Yi X S and Baptista J L 1999 *J. Am. Ceram. Soc.* **82** 3459
[28] Einset E O 1996 *J. Am. Ceram. Soc.* **79** 333
[29] Dullien F A L, El-Sayed M S and Batra V K 1977 *J. Colloid Interface Sci.* **60** 497
[30] Wang H P, Yao W J, Cao C D and Wei B 2004 *Appl. Phys. Lett.* **85** 3414
[31] Egry I 1993 *Scripta Metallurgica et Materialia* **28** 1273
[32] Pan Y and Baptista J L 1998 *J. Eur. Ceram. Soc.* **18** 201
[33] Iqbal K 2016 *Advanced and Refractory Ceramics for Energy Conservation and Efficiency* in *Ceramic Transactions Series* Vol. 256 p. 21